MARMARA UNIVERSITY
FACULTY OF ENGINEERING

THE EFFECTS OF ALTITUDE, SPEED AND MASS FLOW RATE AT AIR INTAKE ON THE AERODYNAMICS OF FIGHTER AIRCRAFT USING OPEN-SOURCE PROGRAMS AND OPERATING SYSTEM

Muhammed Enes TOPCU
Muhammet Enes ŞİRİN

GRADUATION PROJECT REPORT
Department of Mechanical Engineering

Supervisor
Prof. Dr. Emre ALPMAN

ISTANBUL, 2022

MARMARA UNIVERSITY

FACULTY OF ENGINEERING

The Effects of Altitude, Speed and Mass Flow Rate at Air Intake on the Aerodynamics of Fighter Aircraft Using Open-Source Programs and Operating System

by

Muhammet Enes ŞİRİN
Muhammed Enes TOPCU

June 09, 2022, Istanbul

SUBMITTED TO THE DEPARTMENT OF MECHANICAL ENGINEERING IN PARTIAL FULFILLMENT OF THE REQUIREMENTS FOR THE DEGREE

OF BACHELOR OF SCIENCE

AT

MARMARA UNIVERSITY

Signature of Author(s) .....

Department of Mechanical Engineering

Certified By .....

Project Supervisor, Department of Mechanical Engineering

Accepted By .....

Head of the Department of Mechanical Engineering

ACKNOWLEDGEMENT

First of all, we would like to thank our supervisor Prof. Dr. Emre ALPMAN for the valuable guidance and advice on preparing this thesis and giving us moral and material support and Marmara University Mechanical Engineering Department.

June, 2022

Muhammet Enes ŞİRİN

Muhammed Enes TOPCU

CONTENTS

ABSTRACT

The Effects of Altitude, Speed and Mass Flow Rate at Air Intake on the Aerodynamics of Fighter Aircraft Using Open-Source Programs and Operating System

In this thesis, the effect of fighter jet flows with different altitude, speed and air intake on the aerodynamics of fighter jets was investigated. It was also studied from a particular angle of attack. It was also studied from a particular angle of attack. While performing aerodynamic analysis, mostly open-source programs and operating system were tried to use.

Different shock waves were observed in subsonic, transonic and supersonic flows. For this, first of all, some analyzes were made on the F-16 Fighter Aircraft profile. By doing this it was determined that our main solver would be a compressible solver. After that, mesh was created on the GMSH Program, which is a finite element mesh generator. Next, a modified solver was created with rhoSimpleFoam, a compressible solver for fighter aircraft, and simulated in OpenFOAM, a continuum mechanics simulation, at the parameters to be studied.

After completing the 3D analysis, the fighter aircraft was examined under the specified conditions. The results, together with the chosen solver, were compared with NASA's experimental data. Finally, the main purpose is to obtain experimental values and compare the changes in the determined parameters using an open-source programs.

Keywords: Computational Fluid Dynamics, Aerodynamic, Fighter Aircraft, Open Source, OpenFOAM, GMSH

SYMBOLS

C_D : Coefficient of drag force

C_L : Coefficient of lift force

C_m : Coefficient of pitching moment

α : Angle of Attack

ABBREVIATIONS

AFRL : Air Force Research Laboratory

AoA : Angle of Attack

CAD : Computer Aided Design

CFD : Computational Fluid Dynamics

FOAM: Field Operation and Manipulation

NASA : National Aeronautics and Space Administration

VSP : Vehicle Sketch Pad

LIST OF FIGURES PAGE

LIST OF TABLES

1. INTRODUCTION

In this report, it is aimed to examine the effects of fighter jet flows with different altitude, speed, and air intake flow on the aerodynamics of fighter jets by using Computational Fluid Dynamics (CFD) analysis. This examination can be done easily through commercial programs as well as open-source programs. Therefore, while making these analyzes, it is mostly aimed to use noncommercial programs and operating systems. Thus, it is aimed to evaluate the usability of these software in projects without being dependent on widespread commercial software.

1.1. Aerodynamics

Aerodynamics is the study of moving gases passing over a moving body and how they impact the body's movement through the flow. The aerodynamics of a car make it safer and more fuel efficient. It is employed in most vehicles today, especially aircrafts or race cars, because high-speed vehicles require more aerodynamics.

Aerodynamics has played an important role in car racing since the mid-20th century. Later, it started to be used in many fields such as

- aviation
- polymer processing
- power generation
- medical research
- meteorology
- astrophysics

and it continued to improve itself with improved systems from some sectors. Today, its use continues to become widespread in many new fields.

1.2. Computational Fluid Dynamics (CFD)

CFD can study heat transfer, mass transfer, fluid flow, chemical reactions, etc., by solving mathematical equations. used to predict. The result of CFD analysis is engineering data used in redesign, troubleshooting, studies of new designs, and product development. It creates a test and experimental setup and reduces the total effort in the laboratory.

CFD is a sub-branch of fluid dynamics. In CFD, data structures and numerical analysis are used to solve fluid flow problems. At this point, computers are used to visualize fluid flows and solve complex equations used to analyze results. To obtain correct solutions, the user must combine appropriate physical laws and appropriate mathematical equations. It should also define the boundary conditions correctly.

As a computer software of CFD, there are two types of software: One of them is commercial softwares such as Fluent, CFX, StarCD etc. Other one is open source softwares such as SU2, OpenFOAM. In this project, OpenFOAM is used.

1.3. Open-Source Software

Using open-source software has both advantages and disadvantages. Here we can talk about OpenFOAM software. The advantages of using it are more important than the disadvantages.

First, it is completely free, and it is a great advantage that open-source programs do not have any costs, especially since commercial software costs are very high. This saves a lot of money on budget constraints. Another advantage is that it can change the source code at any level of the run and make it better for different situations. Also, in large projects, especially confidential work, commercial software can restrict the project. However, this is not the case with OpenFOAM, the project can be done comfortably and safely.

The disadvantages are the lack of an interface design to use the program easily. Therefore, it is not user friendly. On the other hand, it is not a well-known program. Errors or problems may not be easily fixed. However, bug tracking, and remediation assistance can be obtained by global members of the open community. It should be noted that the advantages of these programs may become more important than their disadvantages.

1.4. F-16 Fighter Aircraft

Fighter aircrafts are military vehicles used to neutralize targets in the air, on land or in the water, to go on reconnaissance flights, and to transport people or weapons. These aircraft are used for attack and defense designed to neutralize their targets by carrying their own weapons.

One of the most common of these aircraft is the F-16 Fighting Falcon. It was developed by General Dynamics as a multi-purpose and single-engine jet fighter aircraft. It was designed as a 4th generation light fighter, proved itself with its extraordinary maneuverability and started to be used by many countries with its success. This aircraft, which made its first flight in 1974 and started to be used 4 years later, is still being used by many countries.

Figure 1. 1: F-16 Fighting Falcon solid model in OpenVSP Hangar

1.5. Literature Review

Aerodynamics of the aircrafts play an important role. It affects almost everything about the aircraft such as design of wings or design of engine intakes. Until today, a lot of studies had been done about F16 or its different configurations with different computational fluid dynamics (CFD) code packages.

For aircraft design, drag optimization is very important for having better flight performance and less fuel consumption. CFD results are analyzed in order to see effects of fuselage and wing in subsonic, transonic and supersonic regimes. At 0.3 Mach, aerodynamic behavior of F-16 at subsonic speeds is observed. At 0.9 Mach, aerodynamic behavior of aircraft at transonic regime is presented and at 1.6 Mach aerodynamic behavior of aircraft at supersonic regime is presented. Fuselage has highest drag contribution due to its high cross section area at subsonic and supersonic speeds. At subsonic regime, viscous drag has more contribution and at supersonic regime, pressure drag has more contribution [1]. In this study drag effects of fuselage, wing and tail sections are analyzed and concluded.

The flow over F-16 which is subjected to different Mach Conditions at subsonic, transonic and supersonic conditions subjecting to turbulent conditions and studying the flow effects at a different angle of attack. The results obtained for C_l, C_d, C_m and the moments on the F-16 Falcon are accurate at the desired cases considered for different Mach (Ma) and angle of attacks (α). The varying of pressure, temperature, and velocity on the surface of the aircraft are clearly studied and are compared with the referred values and seems to be the nearer value

of approaches. The change in velocity with a different angle of attacks was studied and is compared [2].

Other several studies had been done by experimentally [3,4] and numerically [6]. Related aerodynamic characteristics were observed and contributed to literature. C_l, C_d were mainly analyzed experimentally [3] and numerically. Moreover, similar fighter aircrafts were also analyzed [5].

Common challenge was the water-tight geometry and mesh quality. Mesh dependency should be inspected. Lastly, domain of the flow in which F-16 is in it should be appropriate to not affect results such as long enough to not reflect shock waves.

2. METHODOLOGY AND MATERIALS

2.1. Solid Model

The solid model as shown in figure 2.1 is taken from the official website of the open-source software OpenVSP. This software basically offers the opportunity to use real geometry in a computer environment. In addition, it offers the opportunity to change parameters such as wing structure, body structure, etc. on the geometry. Later, the geometry downloaded from the official website was extracted from the mentioned computer software with a solid model extension.

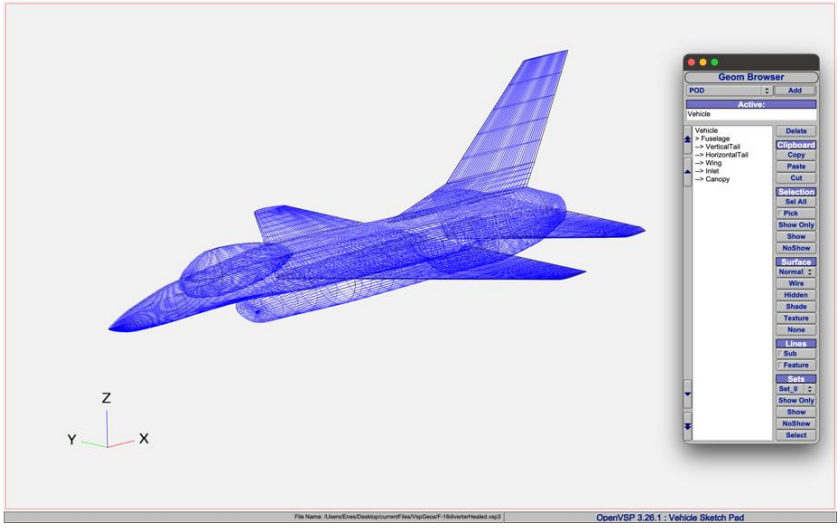

Figure 2- 1: Solid model created in OpenVSP

In this study, since the effect of air intake on aircraft aerodynamics will be examined and the engine air inlet and outlet will be selected as a patch in the simulation environment, a change has been made in the CAD environment. It is appropriate to do this process in open-source software in the same way.

2.1.1. OpenVSP

OpenVSP, also known as Open Vehicle Sketch Pad, is an open-source parametric aircraft geometry tool originally developed by NASA. It can be used to create 3D models of aircraft and to support engineering analysis of those models [7].

2.2. Pre-Processing

The purpose of the mesh is to break down a complex volume into small sizes that the simulation can run. By definition, a mesh can be called a grid of cells and points. It can have almost any shape in any size. It is used to solve Partial Differential Equations (PDE). The history of this technique is closely connected with the history of numerical methods.

2.2.1. Meshing Tools

- Gmsh

Gmsh is an open-source 3D finite element mesh generator with a built-in CAD engine and post-processor. Its design goal is to provide a fast, light and user-friendly meshing tool with parametric input and advanced visualization capabilities. Gmsh is built around four modules: geometry, mesh, solver and post-processing. The specification of any input to these modules is done either interactively using the graphical user interface, in ASCII text files using Gmsh's own scripting language (.geo file) [9].

```
Merge "f16diverter.step";
SetFactory("OpenCASCADE");
//+
Cylinder(2) = {-50, 0, 0, 150, 0, 0, 50, 2*Pi};
BooleanDifference{ Volume{2}; Delete; }{ Volume{1}; Delete; }
//+
Physical Surface("Inlet") = {56};
Physical Surface("Outlet") = {55};
Physical Surface("FarField") = {54};
Physical Surface("F16wall") =
{2,3,4,5,6,7,8,9,10,11,12,13,14,15,16,17,18,19,20,21,22,23,24,25,26,27,28,29,30,31,32,33,34,35,36,37,38
,39,40,41,42,43,44,45,46,47,48,49,50,51,52};
Physical Surface("EngIntake", 136) = {1};
Physical Surface("EngOut", 137) = {53};
Physical Volume("AIR", 138) = {2};
//+
Transfinite Curve {7,35,37,46,80,50,55,61,73,78,48,84,10,105,110,128,26,125,18} = 6;
Transfinite Curve {27,28,29,30,31,40,41,42,43,44,57,64,74,86,90,104,108,113,115,116,118,120,121} = 20;
Transfinite Curve
{16,32,20,21,19,34,24,33,36,22,38,25,39,45,51,52,56,58,56,62,89,67,69,76,77,70,81,82,85,87,92,94,97,98,
5,102,103,106,109,111,127,126,129,130,132,131} = 40;
Transfinite Curve {1,2,3,4,15,17,23,12,14,47,54,63,65,11,71,6,79,91,93,123,133,134,135} = 60;
Transfinite Curve {49,59,60,66,68,72,75,88,95,96,99,100,101,112,117} = 80;
Transfinite Curve {8,9,13,114,119} = 90;
```

Figure 2- 2: Scripting language of Gmsh

As can be seen in the figure 2.2, operations such as domain creation, boolean operation, physical surface naming, and transfinite curve generation have been performed on the .geo file. After the changes on the script file, the file must be reloaded. These operations can also be done from the "Geometry" tab in the interface of the Gmsh program, as seen in the figure 2.3.

After the mesh is received, it can be checked with the checkMesh command over the operating system used by the user in order to check the simulation compatibility.

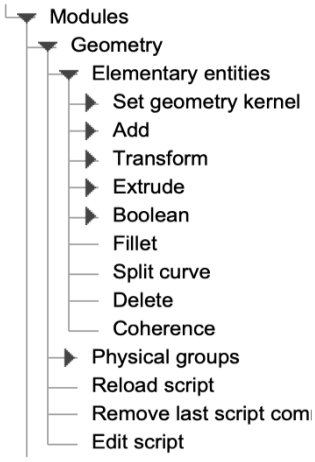

Figure 2- 3 Gmsh operators

- snappyHexMesh

snappyHexMesh is a meshing tool provided with OpenFOAM. Its purpose is to create meshes where hexahedrons are insufficient. It works by clipping the solid model from blockMesh. blockMesh is required for the snappyHexMesh utility to work. blockMesh basically divides the area geometry into groups of 1 or more three-dimensional, hexahedral blocks. The mesh is categorized as a series of cells in each direction of the block [8].

First, the user must create the object to be analyzed. It should be saved in .stl or .obj format. Extensions are available from OpenVSP. The user needs to create a blockMeshDict containing the requested object. However, in complex geometries such as fighter aircrafts, this process can increase the number of cells. The snappyHexMesh tool then inserts the objects by iteratively refining the initial mesh and merging it with the existing mesh [8].

2.2.2. Mesh Generation

The second operation is to create a mesh as shown in figure 2.4. It is important to develop a fine mesh to obtain valid and accurate results. The mesh was created using GMSH, which is open-source software. After importing the geometry into the application, the specified domain was created. While creating the domain, it was considered as cylinder geometry, considering the plane length. For example, 3 plane lengths are set to the front and sides of the geometry, and 5 planes are set to the back of the geometry. Thus, the mesh that will simulate the flow.

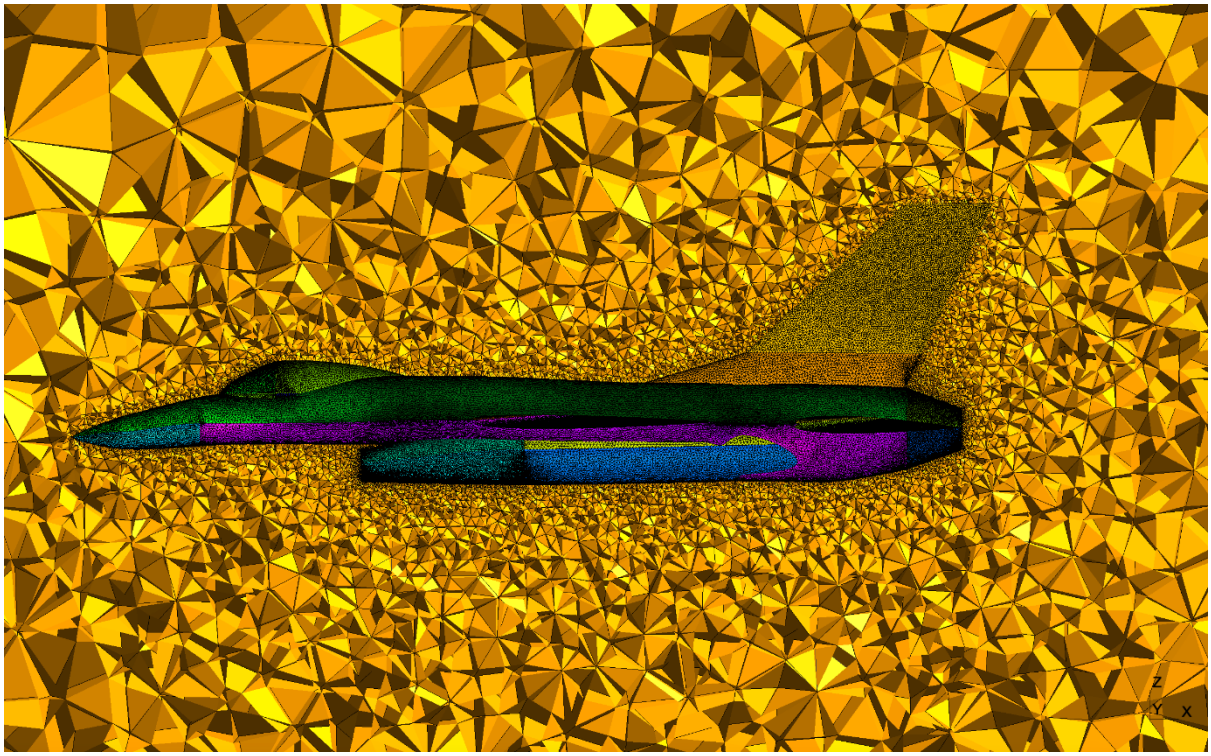

Figure 2- 4: Mesh generation by using Gmsh

Since the flow to be examined is the external flow, the volume of the plane geometry is subtracted from the domain. Then, a thin mesh was formed around the aircraft and a thicker mesh towards the corners of the domain was created to create a suitable environment for the changes that will occur around the aircraft. Also, by doing this, an attempt was made to keep the number of meshes to a minimum.

2.3. CFD Simulation

The flow was simulated in OpenFOAM v8. Before that, the mesh structure of the flow received from Gmsh was read with the gmshToFoam command and then checked with the checkMesh command. The properties of mesh are as in the figure 2.5 below. After the control was confirmed in the program, the models, materials and boundary conditions were determined.

```
Checking geometry...
    Overall domain bounding box (-50 -50 -50) (100 50 50)
    Mesh has 3 geometric (non-empty/wedge) directions (1 1 1)
    Mesh has 3 solution (non-empty) directions (1 1 1)
    Boundary openness (-1.10096e-16 3.28785e-17 -3.46374e-17) OK.
    Max cell openness = 3.1938e-16 OK.
    Max aspect ratio = 18.9624 OK.
    Minimum face area = 5.0118e-05. Maximum face area = 14.1431.  Face area magnitudes OK.
    Min volume = 1.44645e-07. Max volume = 16.3685.  Total volume = 1.17783e+06.  Cell volumes OK.
    Mesh non-orthogonality Max: 79.588 average: 16.7155
   *Number of severely non-orthogonal (> 70 degrees) faces: 8.
    Non-orthogonality check OK.
  <<Writing 8 non-orthogonal faces to set nonOrthoFaces
    Face pyramids OK.
    Max skewness = 1.02257 OK.
    Coupled point location match (average 0) OK.

Mesh OK.

End
```

Figure 2- 5: CheckMesh command result

2.3.1. OpenFOAM

Since OpenFOAM is open-source software, it may come as a difficult package from the beginning. The User's Guide [8] introduces OpenFOAM and information on how the software works through its tutorials. Each application performs a specific task within a CFD workflow. For example, the snappyHexMesh applet is a mesh generator for complex geometry that can create a mesh around a tool. The SimpleFoam application can then simulate steady-state, turbulent, incompressible flow around the vehicle. Also, in OpenFOAM it is possible to run these applications and them in parallel on a single processor or on multiple processors.

- **Case Setup**

OpenFOAM examines the setup of input data files for CFD analysis. The input data includes time information (start time, end time, time step, etc.) and controls for reading and writing data (time, format, compression, etc.). It additionally describes the setting of numerical schemes that affects accuracy and stability of a simulation. Matrix solver controls and algorithm controls are also explained that affect computational time and stability.

- **0 sub-directory**

Once the mesh generation is complete, the user can look at this initial fields set up for this case. The case is set up to start at time t = 0 s, so the initial field data is stored in a 0 sub-directory. The 0 subdirectory contains multiple files, one for each of the fields such as pressure (p), velocity (U), temperature (T) where initial values and boundary conditions need to be set.

Let's examine the p file for the supersonic 2000m altitude case as an example as shown in the figure 2.6:

dimensions

Properties are represented in some chosen units, *e.g.*, mass in kilograms (kg), volume in cubic meters (m^3), pressure in Pascals ($kgm^{-1}s^{-2}$). Algebraic operations must be performed on these properties using consistent units of measurement; in particular, addition, subtraction and equality are only physically meaningful for properties of the same dimensional units. All units are in the Appendix 2-2.

```
17  dimensions      [1 -1 -2 0 0 0 0];
18  internalField   uniform 79584;
19  boundaryField
20  {
21      F16wall
22      {
23          type            zeroGradient;
24      }
25      EngIntake
26      {
27          type            fixedValue;
28          value           uniform 19987;
29      }
30      EngOut
31      {
32          type            zeroGradient;
33      }
34      Inlet
35      {
36          type            zeroGradient;
37      }
38      Outlet
39      {
40          type            fixedValue;
41          value           uniform 79584;
42      }
43      FarField
44      {
45          type            fixedValue;
46          value           uniform 79584;
47      }
48  }
```

Figure 2- 6: The sample of pressure (p) case

internalField

The internal field data which can be uniform, described by a single value; or nonuniform, where all the values of the field must be specified.

boundaryField

The boundary field data that includes boundary conditions and data for all the boundary patches. In this project, 6 boundary conditions are given, the aircraft surface excepting the air intake inlet and outlet named as “F16wall”, the air intake inlet named as “EngIntake”, the engine outlet surface named as “EngOut”, the domain inlet named as “Inlet”, the domain exit named as “Outlet”, and the lateral surface of the domain named as “FarField”.

2.3.2. Turbulence Models

Changes in flow direction are always so slow that turbulence can adjust itself to local conditions. In flows where convection and diffusion cause significant differences between the generation and elimination of turbulence, e.g. In recirculating flows, a compact algebraic solution for the mixing length is no longer possible. The way forward is to consider statements about the dynamics of turbulence. The k–ε model focuses on the mechanisms that affect turbulent kinetic energy.

It is noted that the results of the k–ε model are much less sensitive to the assumed values in free flow, but its near-wall performance is not satisfactory for boundary layers with reverse pressure gradients. This leads to the proposition of a hybrid model using the transformation of the k–ε model to a k–ω model in the near-wall region and the standard k–ε model in the fully turbulent region away from the wall. The Reynolds stress calculation and k-equation are the same as in the k–ω model, but the ε-equation is converted to a ω-equation by replacing ε = kω.

The turbulence models tried for this flow were the k-ε model and the k-ω SST. Since the entire flow is compressible, the solvent was density-based. Also, all simulations are compressible, energy equations are solved to solve the flows.

2.3.3. Materials

The working fluid in this simulation was an ideal gas because the "Pressure Far Field" boundary condition could be compressed with it. The environment for the flight of the F-16 aircraft has been adjusted to the conditions of the world atmosphere model. Earth atmosphere model data were obtained from the equations found on the official website of NASA [10]. The F-16 fighter aircraft can ascend to a maximum of 50000 feet. The related equations are as follows.

$$\begin{gathered} For\ 11000 < h < 2500\ (Lower\ Stratosphere) \\ T = -56.46 \\ p = 22.65e^{1.73-0.000157h} \end{gathered} \tag{2.1}$$

$$\begin{gathered} For\ h < 11000\ (Troposphere) \\ T = 15.04 - 0.00649h \\ p = 101.29\left[\frac{T + 273.1}{288.08}\right]^{5.256} \end{gathered} \tag{2.2}$$

where h = altitude (m) and T = temperature (°C). The code for the calculations using Equation 2.1 and Equation 2.2 is in the Appendix 2-3.

2.3.4. Boundary Conditions

Pressure far-field boundary conditions were used in this simulation to model a free-stream compressible flow at infinity, with free-stream Mach number and static conditions specified. The aircraft was given with "wall" boundary condition.

Table 2.1. Boundary conditions of patches

BOUNDARY CONDITIONS	
Domain Inlet	*velocity Inlet (U)*
Engine Outlet	*mass Flow Inlet*
Domain Outlet	*fixed Pressure (p)*
Air Intake	*fixed Pressure (p)*
Far Field	*freestream*
F16	*wall*

- **Secant Method**

Since the mass flow rate is given to the engine outlet as boundary conditions, it is necessary to calculate the pressure in the air intake. Since the value could not be calculated easily. Therefore, Secant Method [11], which is a root finding method, was used. The formula is

$$x_{i+1} = x_i - \frac{f(x_i)(x_{i-1}-x_i)}{f(x_{i-1})-f(x_i)} \tag{2.3}$$

where $x_i =$ pressure (Pa) and $f(x) = \dot{m}_{in} - \dot{m}_{out}$. The $\dot{m}_{out}$ is known since the mass flow rate is given to the engine outlet.

In order to use this method, first of all, the engine outlet conditions are to estimate the air intake pressure value to the file. When the values start to converge after starting the simulation, the air intake pressure is reduced from the p file in the 0 sub-directory folder. Then, when the simulation is restarted and converged, it is stopped. After opening in ParaView with "paraFoam" command, the Extract Block filter is selected. Then the Extract Surface filter is

selected, and the air intake and engine outlet surfaces are marked. Add the Generate Surface Normal filter and open the Calculator. The mass flow rate, $m = \rho VA$, is calculated in the Calculator and the Integrate Variables filter is selected to integrate the variables. The results of the integrated variables are output as tables. The $f(x)$ value in the formula is obtained from the result, and when it is put into the secant method formula, the next airway pressure is calculated as it converges to its real value.

2.3.5. Solution

The solver was the semi-closed method for the pressure dependent equations (SIMPLE) algorithm. This algorithm is an iterative procedure to solve the velocity and pressure equations for steady state. The pressure equation and relaxation factors for the area are set to 0.3, for the velocity field to 0.6, and for the turbulent kinetic energy, the turbulent propagation velocity and energy are set to 0.2. Convergence during solution was checked manually with force coefficient values instead of convergence control over residuals. The data is printed and plotted on the lift, drag and moment coefficients and residuals for the solution variables.

2.3.6. Reference Values

The reference values should be given to get the actual results when the force coefficients are calculating. These reference values vary according to altitude, Mach and angle of attack. In this software, reference values are written to a file named "controlDict" in the system folder. The section of functions is opened in the file and a section of forces is created under it. As seen in the picture, the plane in the flow, namely "f16wall", is written as patch. Then, rhoInf, liftDir, dragDir, pitchaxis, magUInf, lRef, and Aref values are changed and written according to the situation. For example, it is adjusted according to the supersonic and $\alpha = 10°$ as

```
functions
{
    forces
    {
        type            forceCoeffs;
        libs            ("libforces.so");
        writeControl    timeStep;
        writeInterval   1;

        patches
        (
            F16wall
        );

        log         true;
        rhoInf      1;
        CofR        (1 0 0);
        liftDir     (-0.1736579192 0 0.984863);
        dragDir     (0.984863 0 0.1736579192);
        pitchAxis   (0 1 0);
        magUInf     410;
        lRef        8.5;
        Aref        65;
    }
}
```

Figure 2- 7: The functions part of control dictionary

shown in the figure 2.7. lRef and Aref values represent the distance to the center of gravity of the aircraft and the top view area, respectively*(**Appendix 2-3**)*.

2.3.7. Iterate

The number of iterations was adjusted according to the convergence criterion and the complaint of the residuals. The criterion is given as 10^{-3}. Simulations were stopped when the observations in the graphs of Lift vs. Iterations and Drag vs. Iterations converged.

2.4. Post-Processing

There are two principal possibilities for post processing in OpenFOAM. First, there are tools that are executed after a simulation has finished. This tools work on the written data of the solution sample and ParaView are two examples for such tools.

Besides that, there is run-time post processing. Run-time post processing performs certain operations on the solution data as it is generated. Consequently, run-time post processing allows for a much finer time resolution. The functions, e.g., for calculating forces or force coefficients are an example for run-time post processing. The big disadvantage of this method is, that the user has to know the intended post processing steps before starting a simulation.

2.4.1. ParaView

ParaView is a graphical post-processor [12]. This program is called by invoking the command paraFoam. paraFoam is a script that calls ParaView with additional OpenFOAM libraries. Besides viewing and post-processing simulation results, ParaView can be used to view the mesh. When refining a mesh, it is important to check neighboring cells for the transition of mesh fineness. Figure 3.2 shows an example how ParaView displays a mesh.

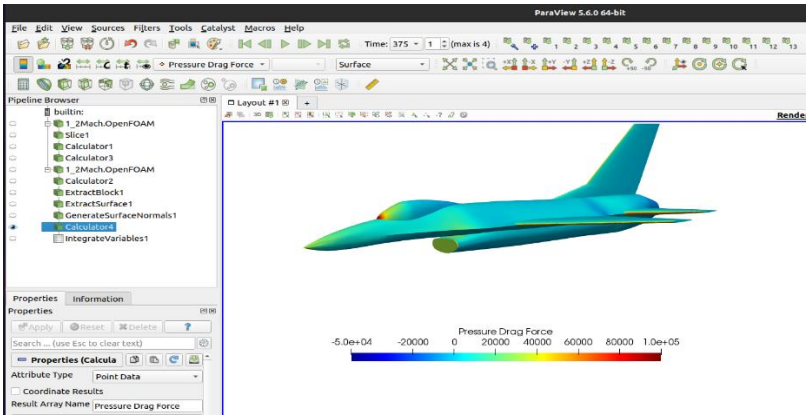

Figure 2- 8: ParaView interface and filters that are used for this project

In addition, areas such as pressure, speed and temperature can be seen around the aircraft. Longitudinal sections of 2D planes or 3D stream tracers can be taken from the tab at the top of the Pipeline browser. It is then possible to calculate the Lift and Drag Forces on the aircraft surface using the filters as shown in the figure 2.8. It is possible to visualize these forces, Mach field etc. using the calculator in the same tab.

3. RESULTS AND DISCUSSION

In this section, the collected data are compared according to the purpose of the research. First, mesh independency was examined. The obtained data are then compared with reliable experimental data. The purpose of this is to prevent the results from being meaningless with any errors. Then, the effects of altitude, Mach, angle of attack, and mass flow rate at the air intake, which are the purpose of this study, on the drag were analyzed.

3.1. Mesh Independency

It is necessary to make sure that the solution is also independent of the mesh resolution. Not checking for this is a common cause of erroneous results in CFD and this should be done at least once for each type of issue being dealt with so that the same mesh sizing can be easily applied the next time a similar issue occurs. In this way, the results are more reliable.

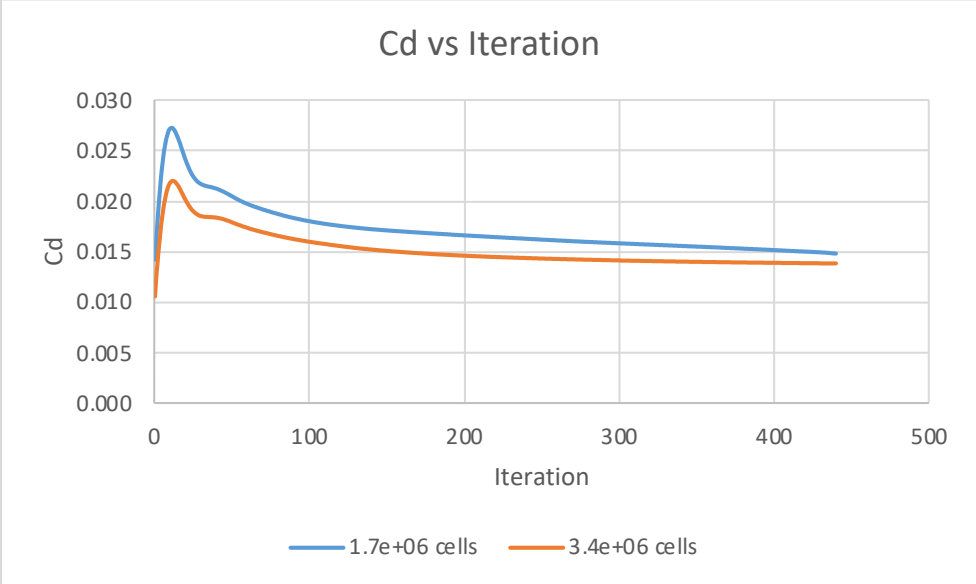

Figure 3. 1: Cell number effects on convergence of C_d

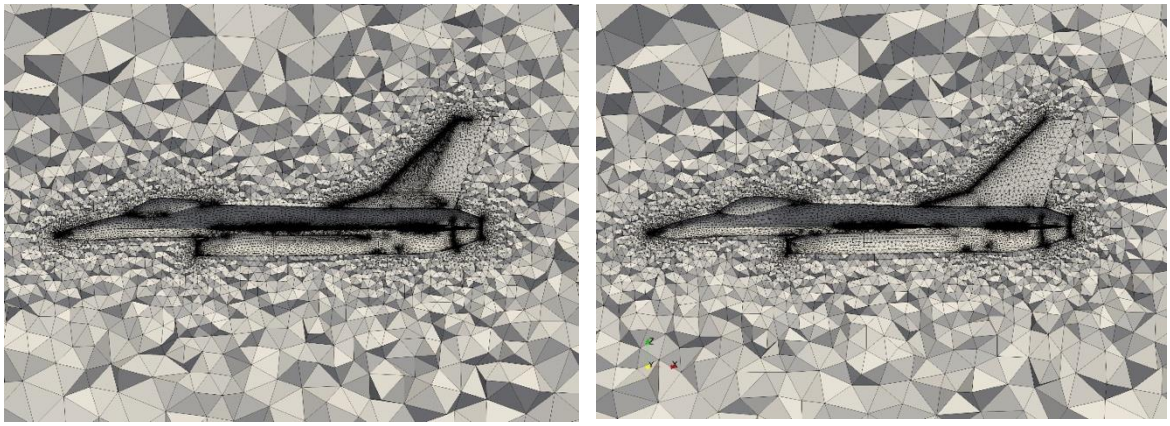

a *b*

Figure 3. 2: 3.4 million cells (*a*) and 1.7 million cells (*b*)

Table 3. 1: Cell numbers with converged C_d values

Number of Cells	Drag Coefficient
3.4 million	0.01381
1.7 million	0.01485

$$Error_{mesh\ related} = \frac{0.01485 - 0.01381}{0.01485} \times 100 = 7.1\%$$

Simulations were taken according to different cell numbers. The associated margin of error was calculated, and it was decided that the error would not affect the results much. In addition, with this decision, it became an advantage in terms of time management.

3.2. Comparison with NASA

It is important to validate the outputs from the project with a reliable source. Project outputs may not show realistic results due to issues such as user error, lack of resources, etc. during the project construction phase. It is not possible to be completely sure about the reliability of research, articles or theses that have been done similar to this project before. Therefore, the data collected in this study were compared with the highly reliable "Aerodynamic Characteristics of Forebody and Nose Strakes Based on F-16 Wind Tunnel Test Experience"[y] study conducted at a NASA-contracted research center.

The study was conducted under similar conditions with that study. The converging drag and lift coefficient values are as follows.

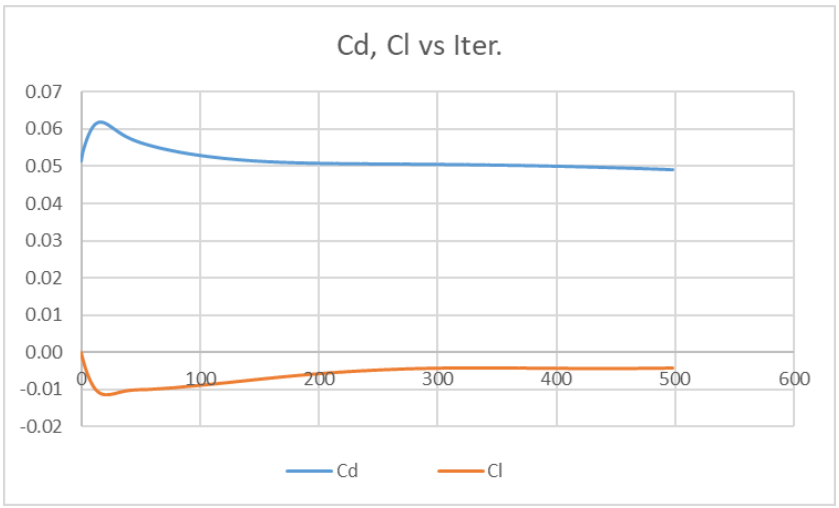

Figure 3. 3: Converging C_d, C_l values to compare NASA

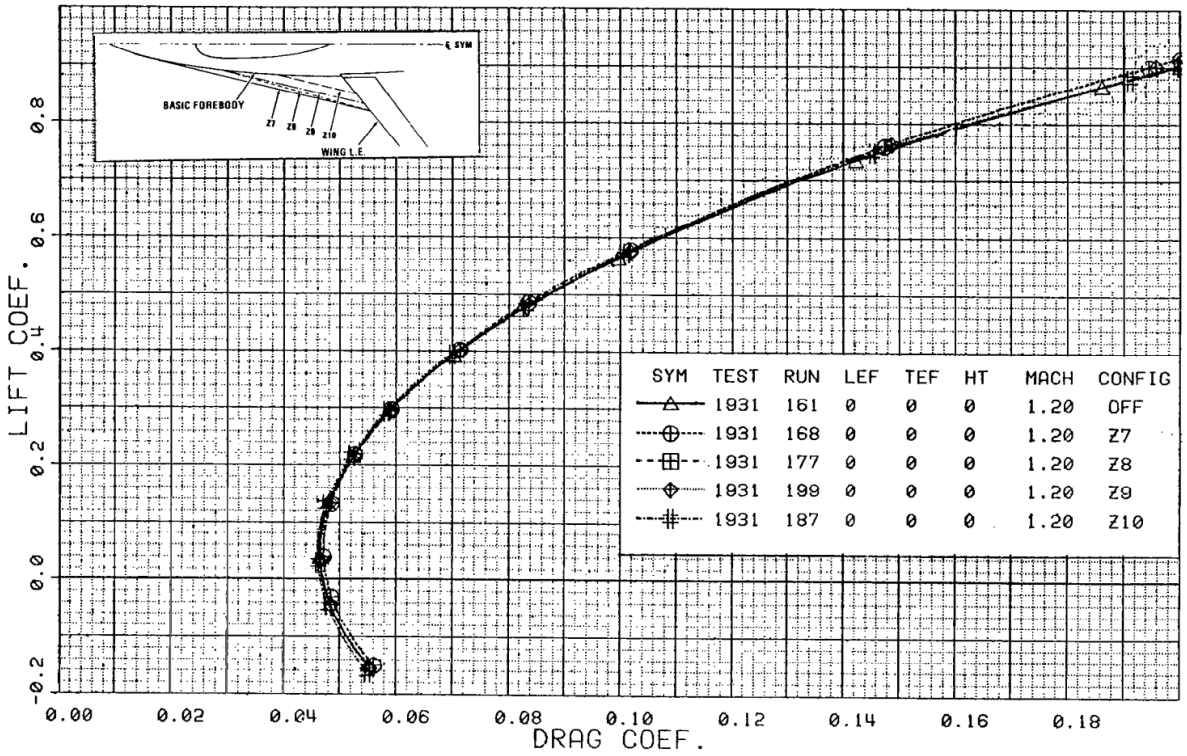

Figure 3. 4: NASA wind tunnel experiment result [3]

Simulation results for C_d, C_l and NASA experiment results [3] are tabulated in following table.

Table 3. 2: Comparison with NASA wind tunnel test

	Cd	**Cl**
NASA Research	≈ 0.048	≈ -0.004
This Study	0.04911	−0.00429

3.3. Altitude Effects

To examine altitude effect on drag coefficient (C_d) three different altitude is selected. F16 is simulated at 2000, 4000 and 6000 meters altitude with 1.2 Mach speed. Figure 3.5 shows the altitude effect on the C_d. It is decreases by altitude with respect to simulated results. Convergence of the simulations considered C_d value instead of residuals. Figure 3.6 shows C_d change over iteration.

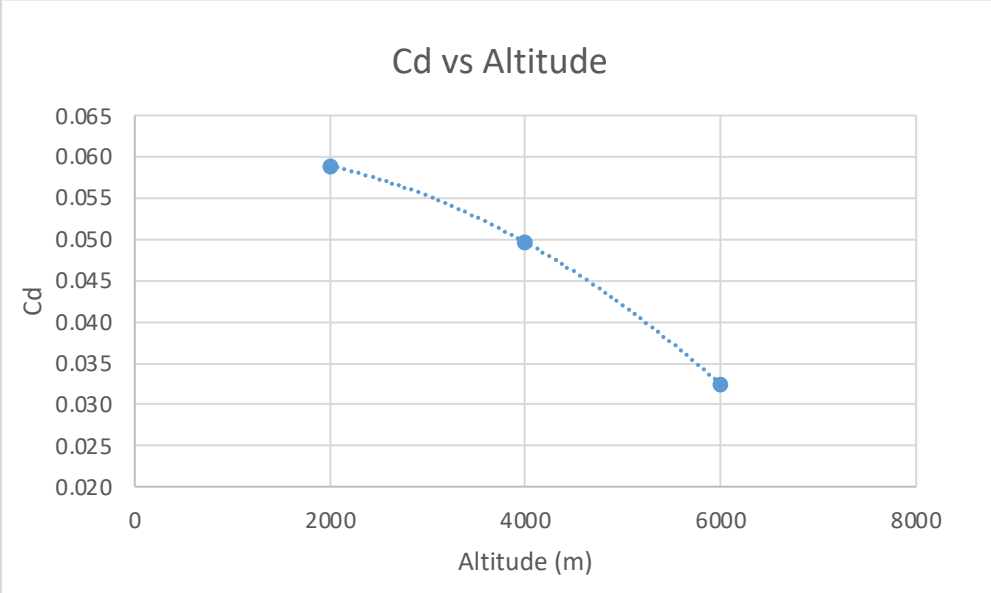

Figure 3. 5: C_d change with respect to altitude

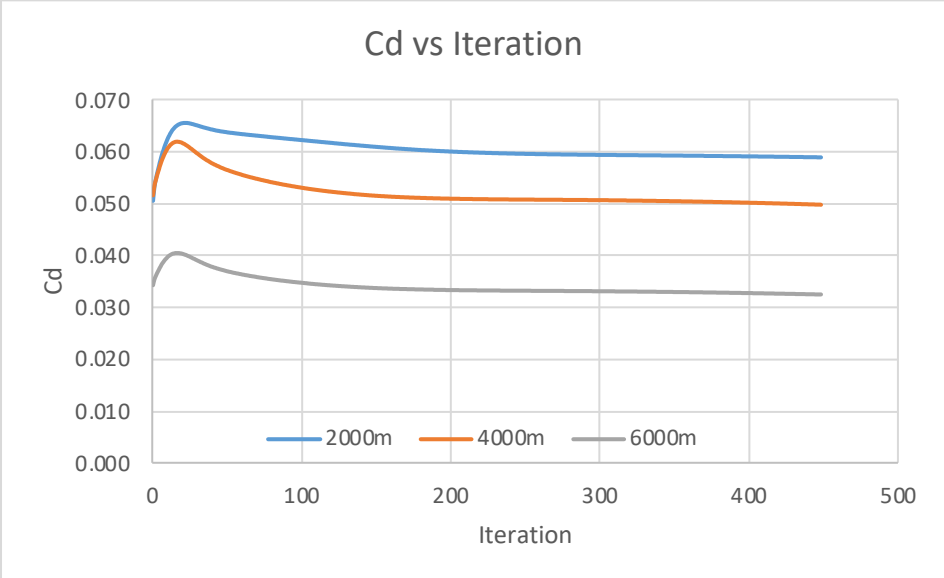

Figure 3. 6: C_d versus iteration at different altitudes

Gage pressures acting on F16 are shown in the figure 3.7. Gage pressure decrease can be clearly seen in the figure 3.7 with respect to altitude. Diverter region of the aircraft (upper region of engine inlet) has very high pressure due to compression of air in that region. However, diverter region does not affect the drag force according to figure 3.8.

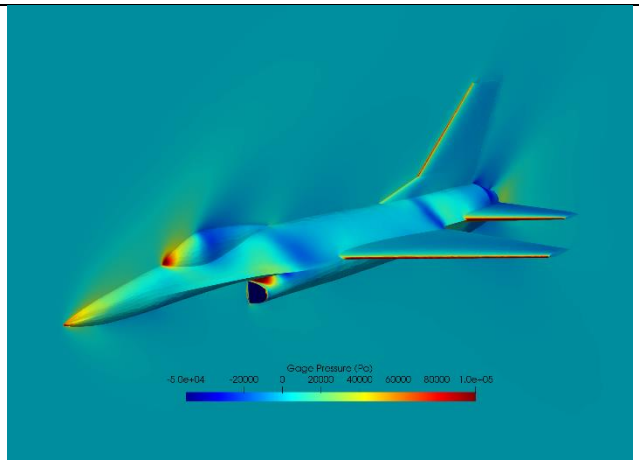

a

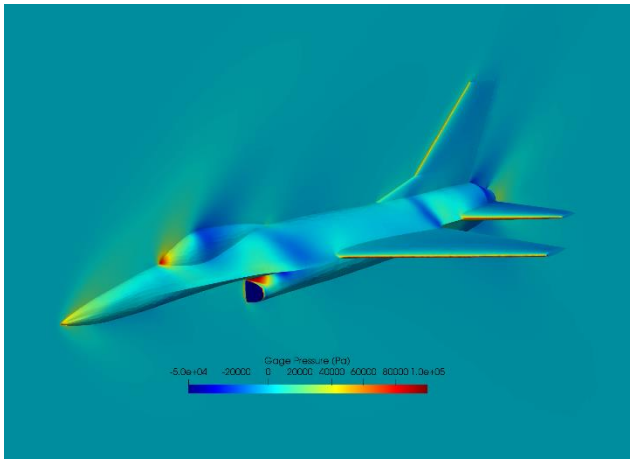

b

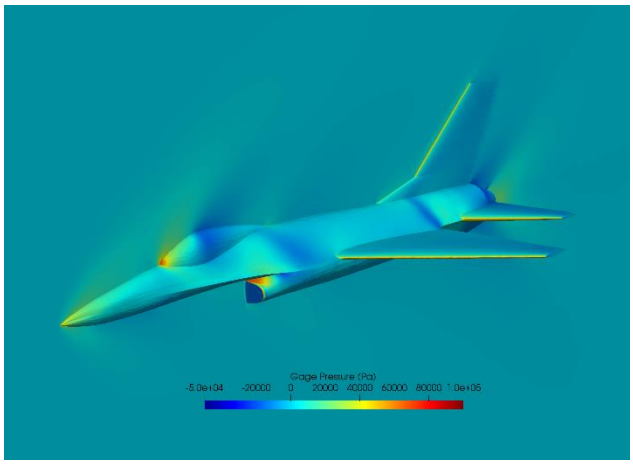

c

a : 2000 meters *b*: 4000 meters *c*: 6000 meters

Figure 3. 7: Pressure distribution on F16 at different altitudes

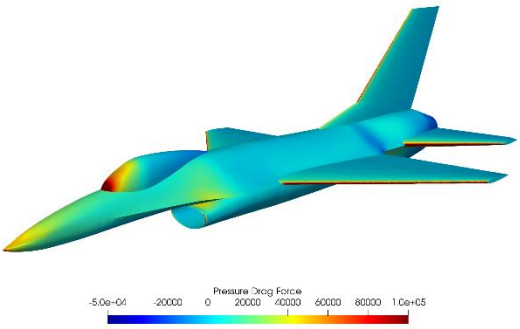

a

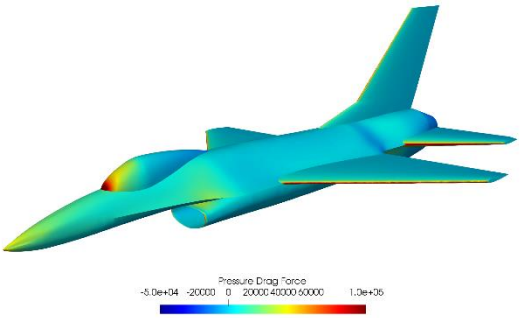

b

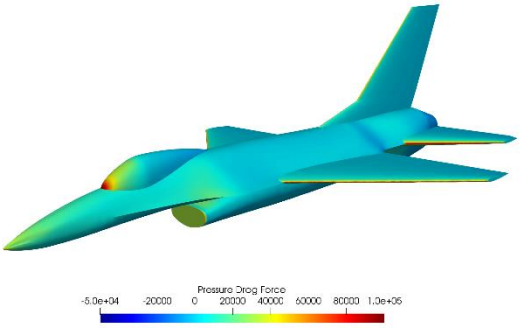

c

a : 2000 meters *b*: 4000 meters *c*: 6000 meters

Figure 3. 8: Drag force distribution on the F16 at different altitudes

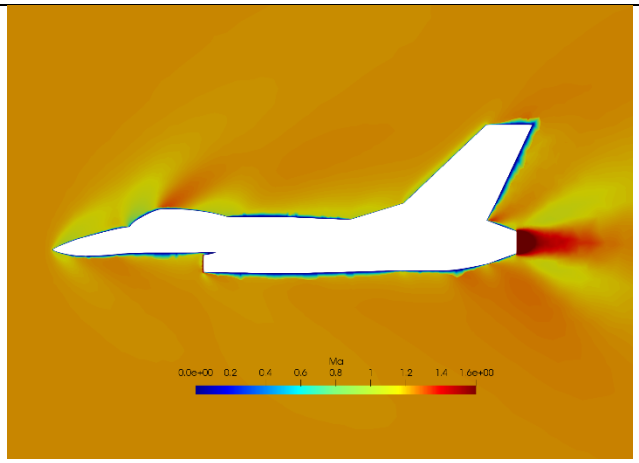

a

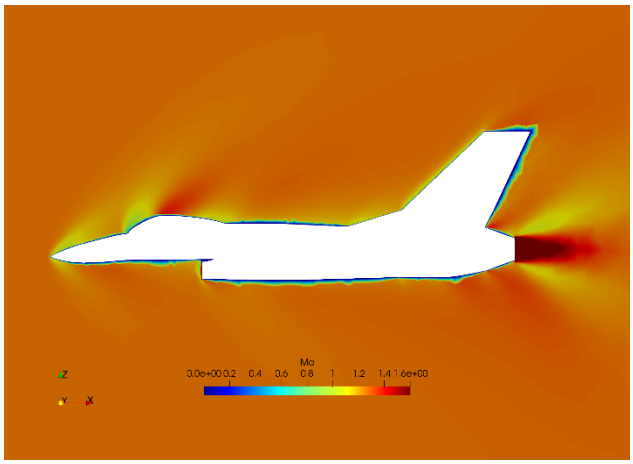

b

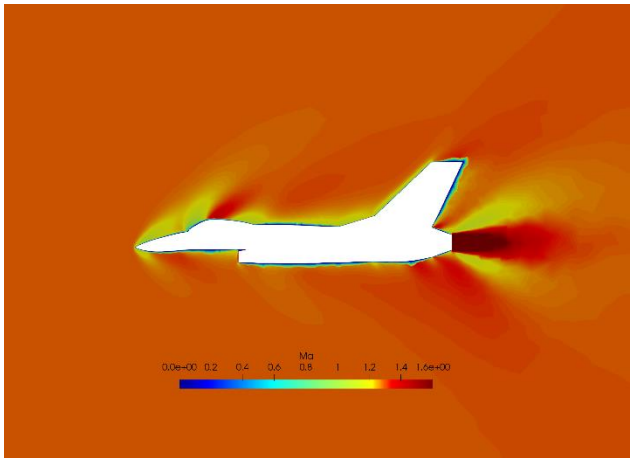

c

a : 2000 meters *b*: 4000 meters *c*: 6000 meters

Figure 3. 9: Flow speed as Mach number over F16 side view at different altitudes

3.4. Mach Number Effects

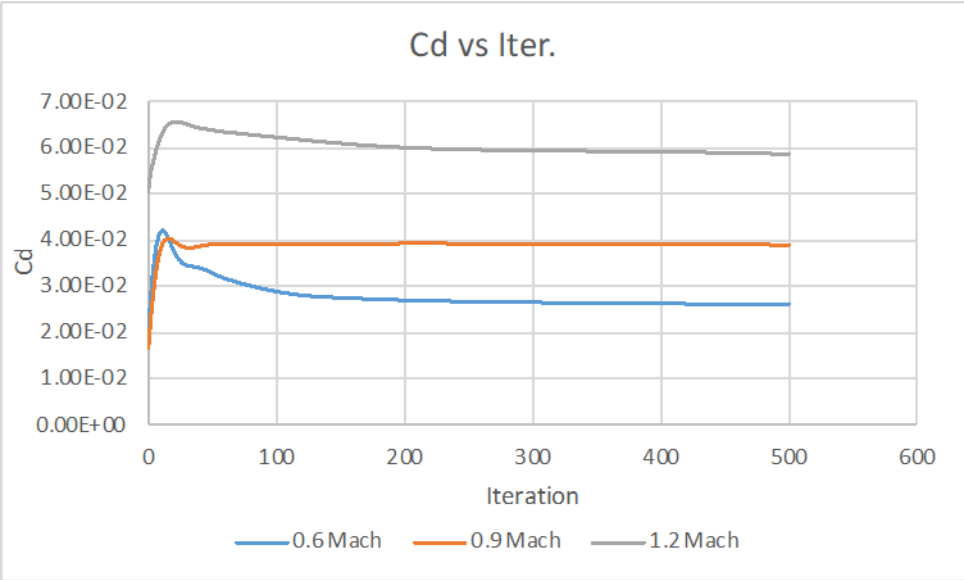

Figure 3. 10: C_d versus iteration at different Mach numbers

To examine Mach number effect on the C_d three simulations were run. Instead of residuals, C_d values considered to converge. Figure 3.10 shows that C_d has converged approximately 300 iterations.

Increasing the speed of aircraft has C_d increased as shown in the figure 3.11. Subsonic flow does not create shock waves so pressure distribution on the aircraft does not show dramatic change.

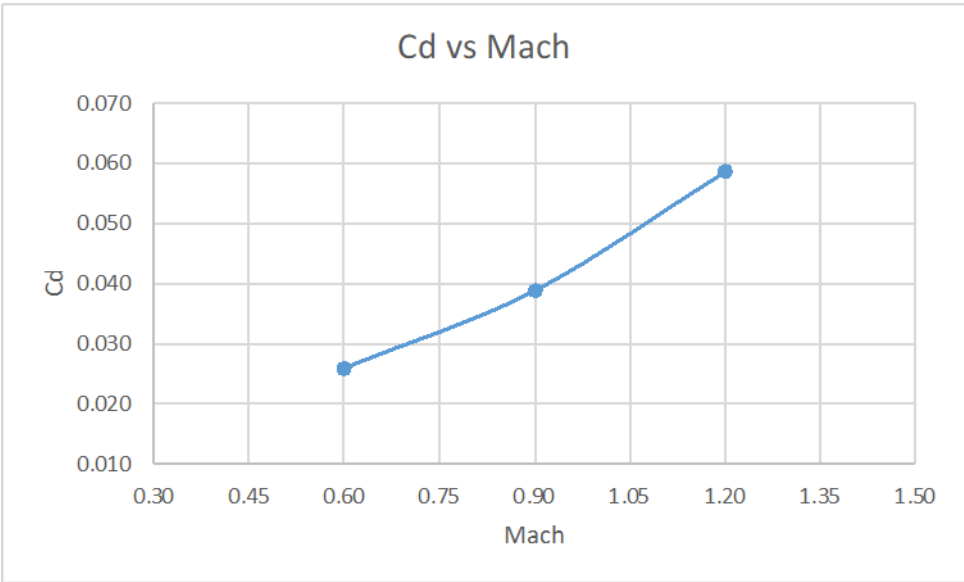

Figure 3. 11: C_d change with respect to Mach number

At supersonic speed, shock waves occur on the aircraft at nose and on cockpit. Shock waves can be distinguished in the figure 3.12 and figure 3.14. Shock waves create sudden change in pressure and that pressure change affects drag force. In the figure 3.13, pressure sourced drag force has increased on cockpit at supersonic flight.

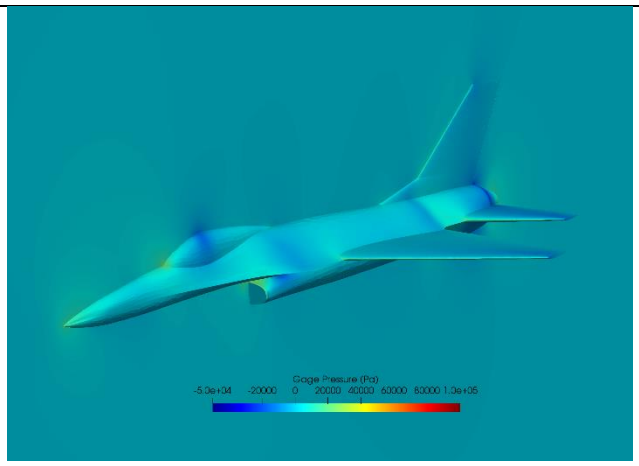

a

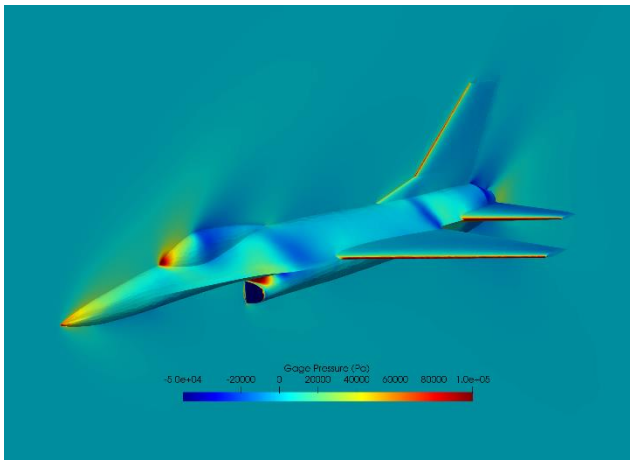

b

a : 0.6 Mach *b*: 1.2 Mach

Figure 3. 12: Pressure distribution on F16 at different Mach numbers

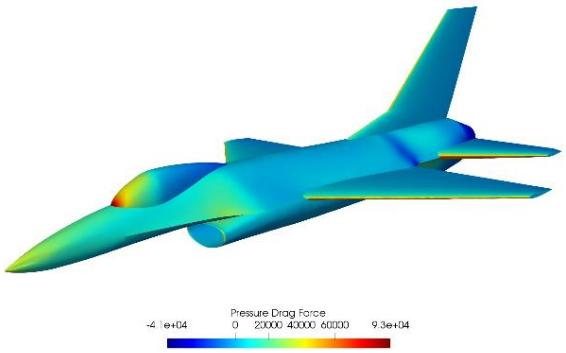

a

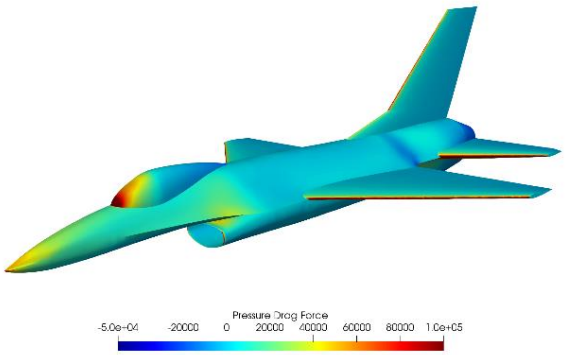

b

a : 0.6 Mach *b*: 1.2 Mach

Figure 3. 13: Drag force distribution on the F16 at Mach numbers

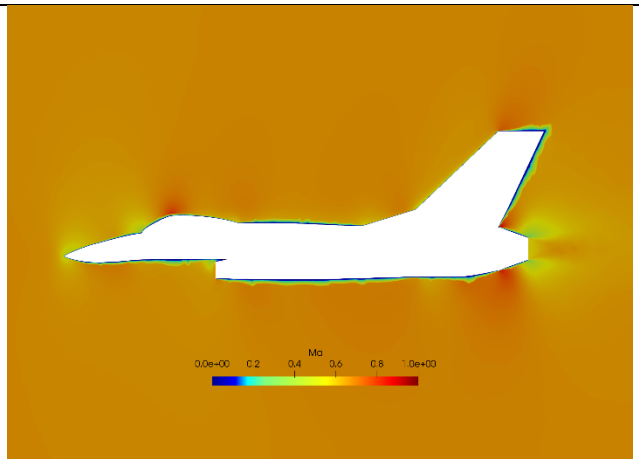

a

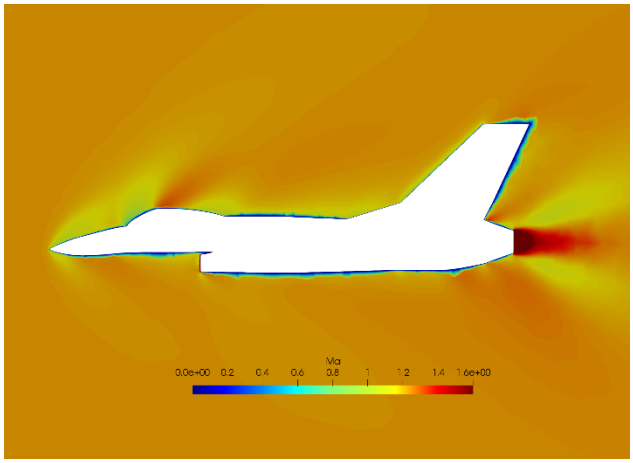

b

a : 0.6 Mach *b*: 1.2 Mach

Figure 3. 14: Flow speed as Mach number over F16 side view

3.5. Angle of Attack Effects

F16 flight conditions at 2000 m altitude with 1.2 Mach speed are simulated with different angle of attacks (AoA). Coefficient of drag, C_d, coefficient of lift, $C_{l,}$ and has converged and shown in the figure 3.15 and figure 3.17 respectively.

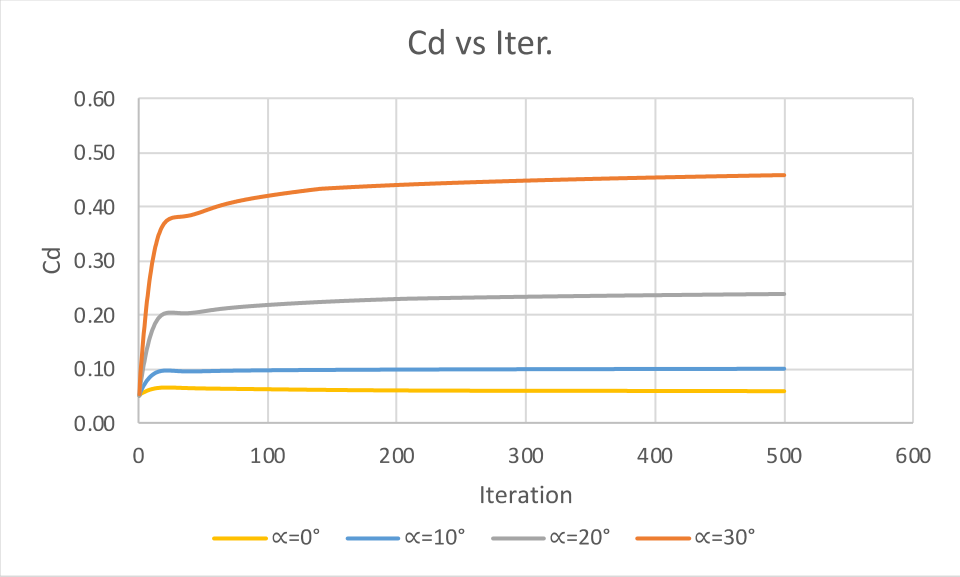

Figure 3. 15: C_d versus iteration at different Angle of Attacks

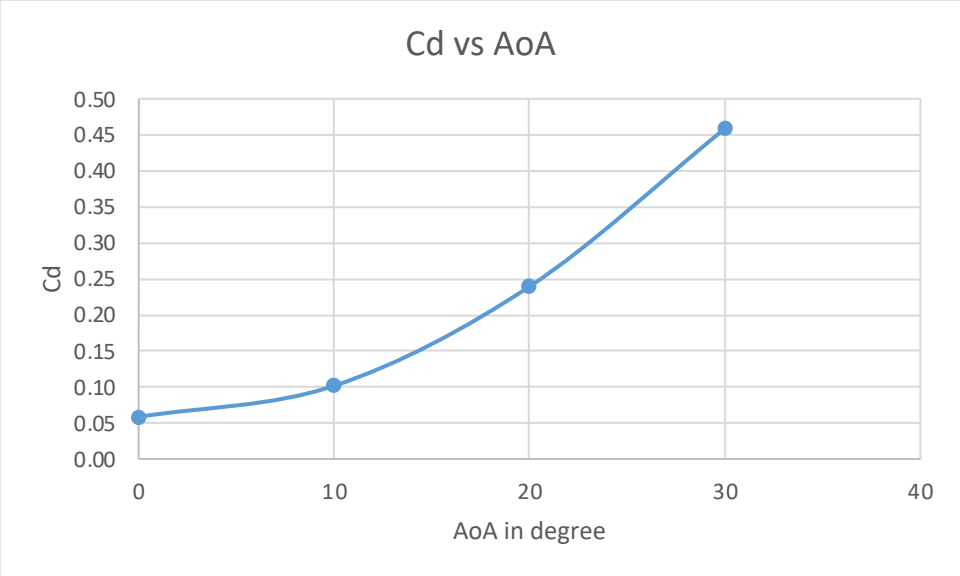

Figure 3. 16: C_d change with respect to Angle of Attack

Figure 3.16 show C_d change with increasing AoA. Polynomial increment trend can be easily observed in the figure. This trend can be interpreted as the aircraft has to produce more thrust while taking off so fuel consumption increases.

On the other hand, C_l also increases with respect to increasing AoA figure 3.18 shows the behavior of C_l. Slope of the line decreased after 20° AoA. Polar drag curve is in the figure 3.19 and represents more comprehensive observation.

Pressure distribution of the aircraft are in the figure 3.21. Increasing AoA creates more negative pressure on the upper part of the aircraft and high pressure on the bottom part. Higher

AoA creates higher pressure difference between upper and bottom parts of the aircraft. Moreover, drag force acting on the aircraft has changed and can be seen in the figure 3.23.

Pressure tends to create flow high pressure to low pressure as naturally and creates force of the aircraft. Air flows faster in low pressures and this can be observed in the figure 3.22 with respect to AoA.

Air flow at 20° AoA were visualized and shown in the figure 3.20 for better understanding of the result in figure 3.22.

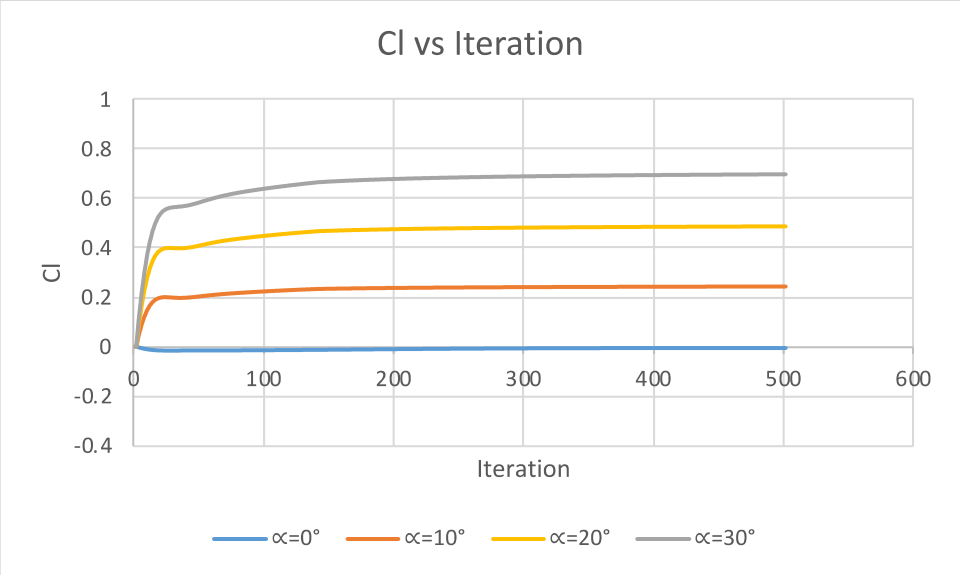

Figure 3. 17: C_l versus iteration at different Angle of Attacks

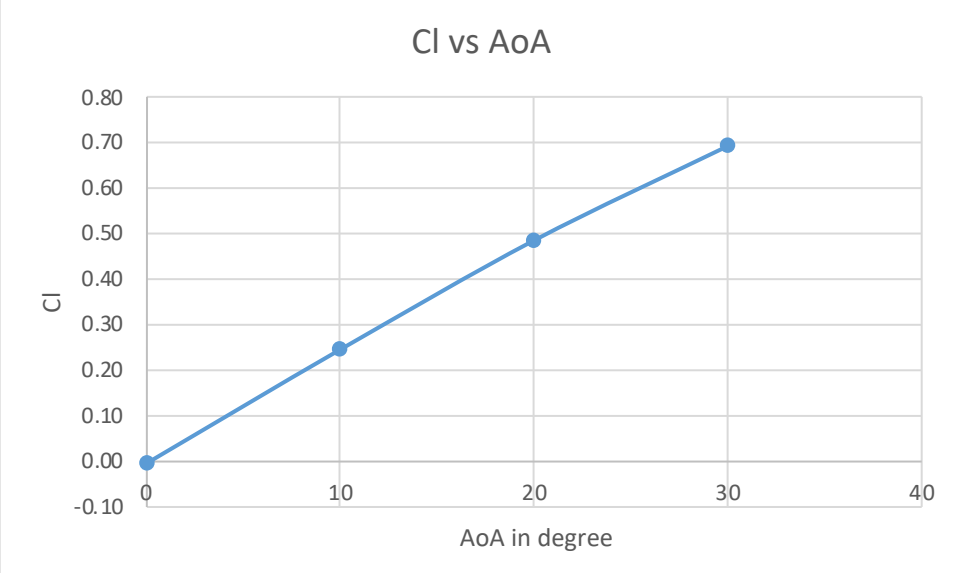

Figure 3. 18: C_l change with respect to Angle of Attack

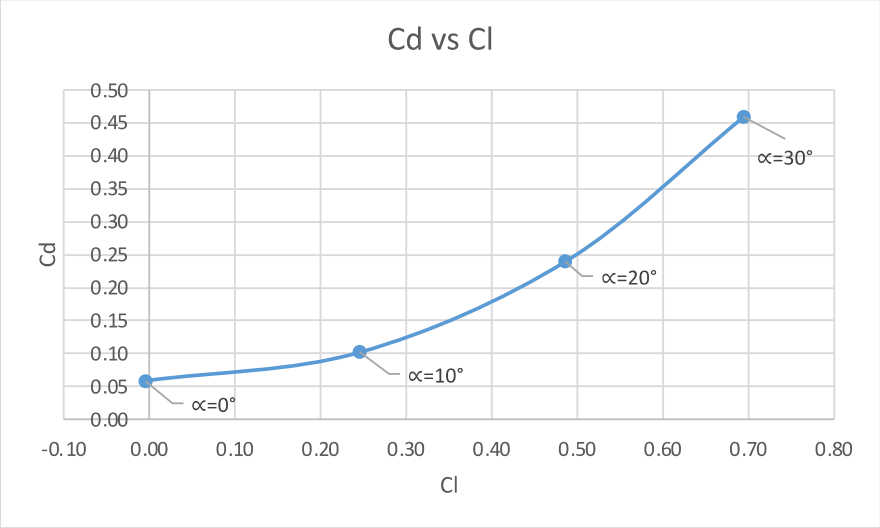

Figure 3. 19: Polar drag curve

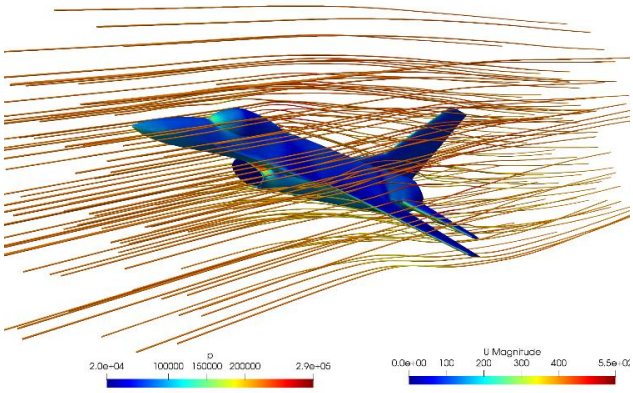

a

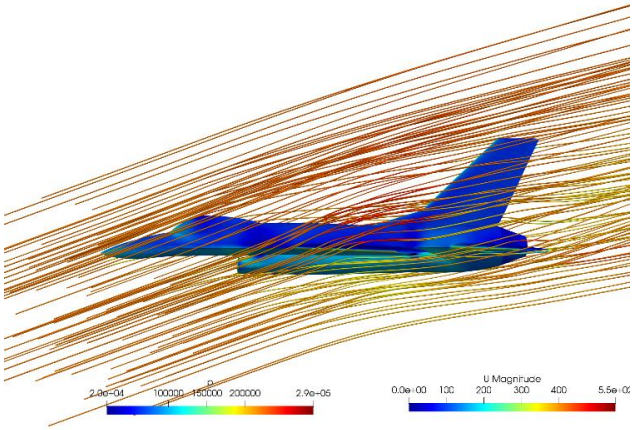

b

a: viewpoint 1 *b*: viewpoint 2

Figure 3. 20: Air flow over F16 at 20° AoA

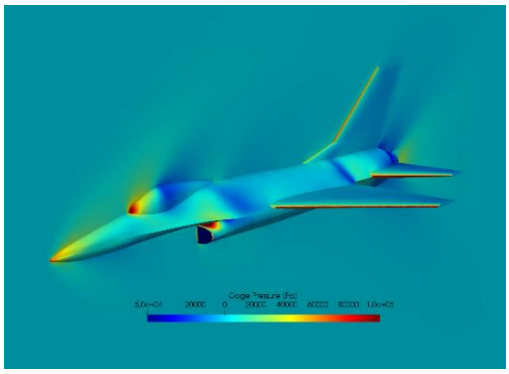

a: α=0°

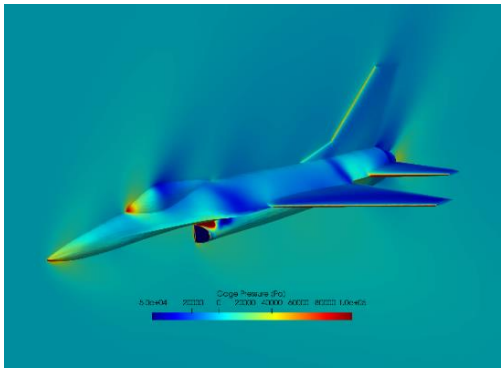

b: α=10°

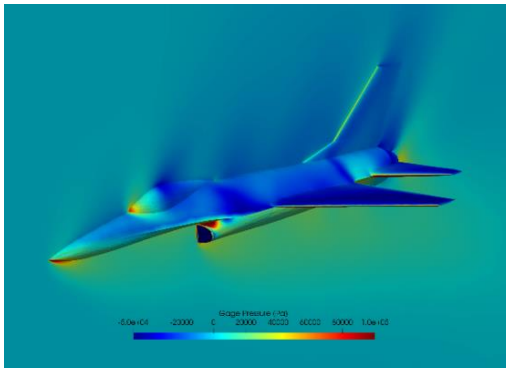

c: α=20°

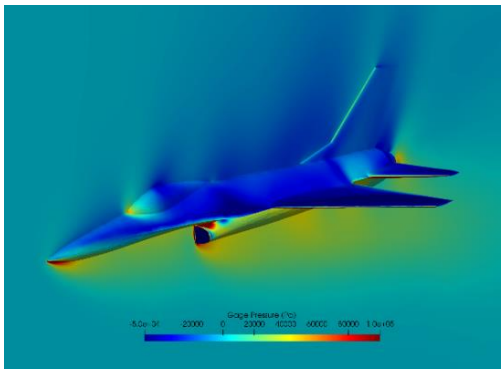

d: α=30°

Figure 3. 21: Pressure distribution on F16 at different Angle of Attacks

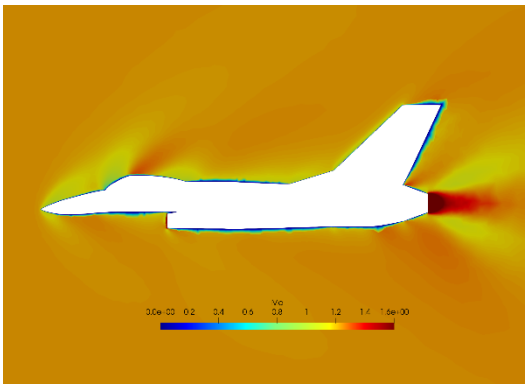

a: α=0°

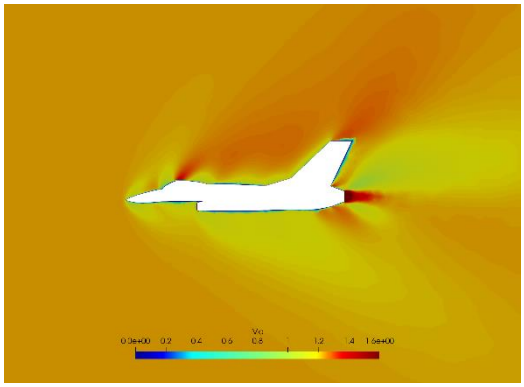

b: α=10°

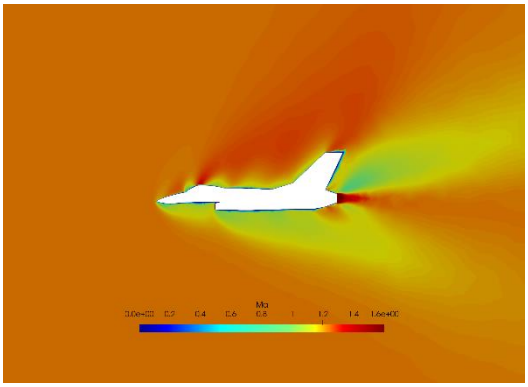

c: α=20°

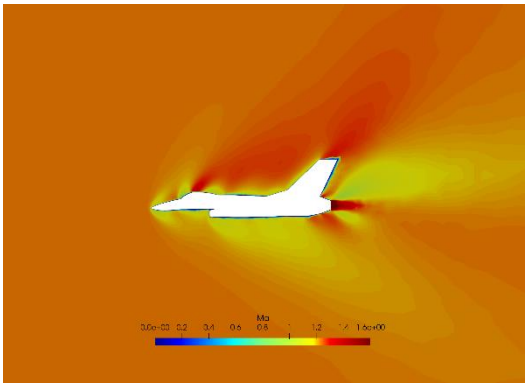

d: α=30°

Figure 3. 22: Flow speed as Mach number over F16 side view at different AoA

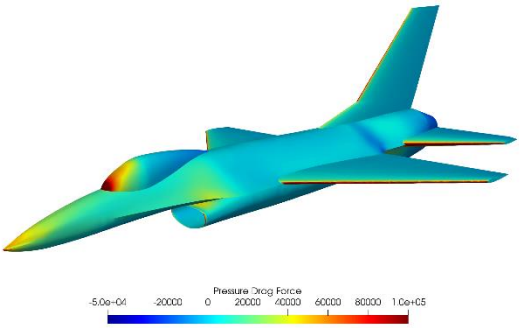

a

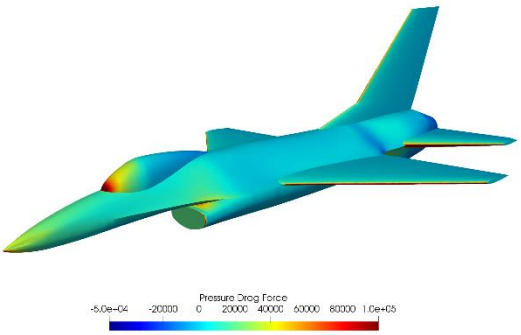

b

a : α=0° *b*: α=20°

Figure 3. 23: Drag force distribution on the F16 at two different AoA

3.6. Engine Air Inlet Mass Flow Rate

F16's engine inlet and outlet are closed to analyze mass flow inlet effect on the aircraft's C_d. Simulations were run until C_d values were converged at 2000m altitude and 0.6 Mach speed. C_d values are plotted with respect to iteration in the figure 3.24.

Pressure distributions on the aircraft are visualized as gage pressure and shown in the figure 3.25. Pressure on the engine intake of the aircraft stops flow in closed case and pressure slightly increases at that section. In open case, low pressure is created for air intake, so mass enters the engine. In closed case air is blocked to enter the engine and difference can be observed in figure 3.26.

To compare more realistically, C_d is calculated without engine inlet and outlet surfaces and C_d is higher than closed case that the engine inlet and outlet are closed. Figure 3.27 is inadequate to show more clearly. Even though drag force change could not be visible easily, numerical result was not same. It can be interpreted from converged C_d values.

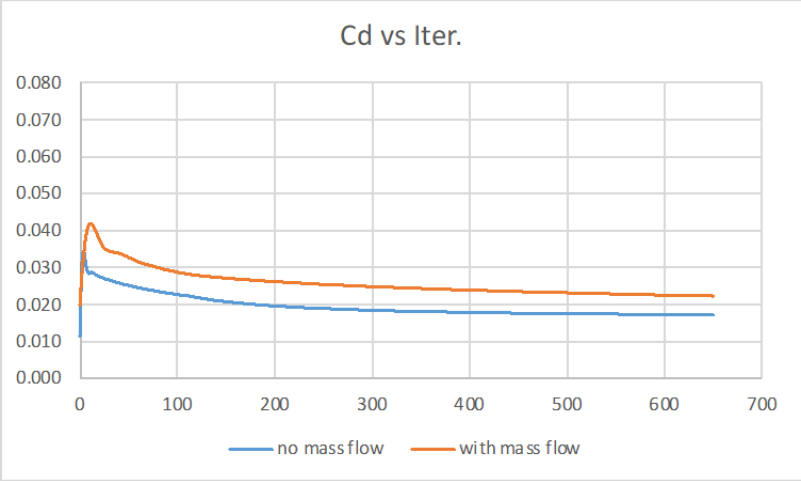

Figure 3. 24: C_d versus iteration at two different engine intake condition

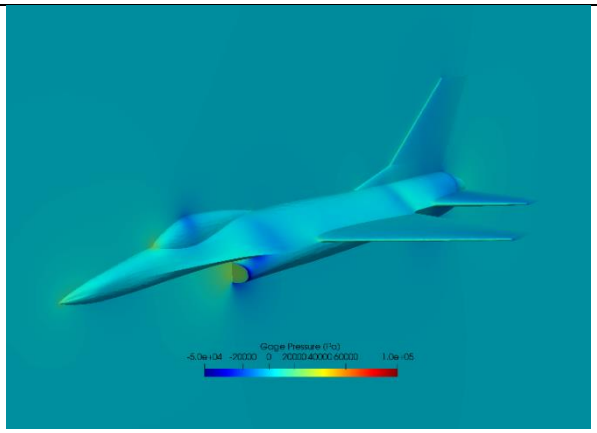

a

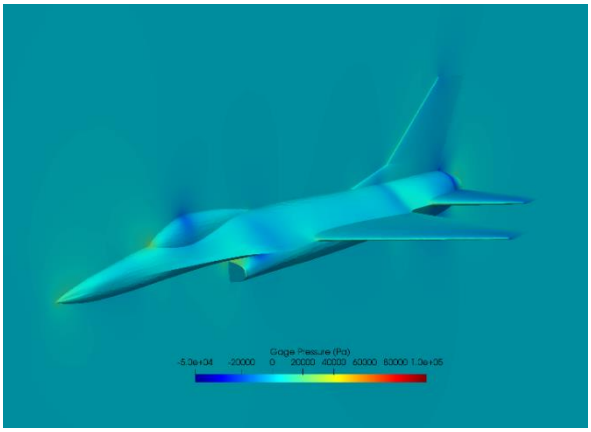

b

a : engine intake closed (no mass flow) *b*: engine intake open (with mass flow)

Figure 3. 25: Pressure distribution on F16 at different engine intake conditions

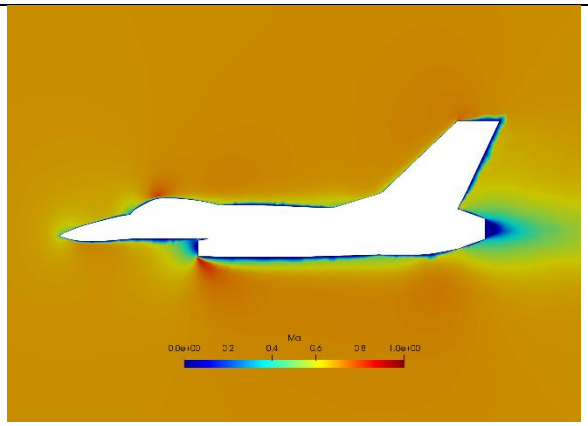

a

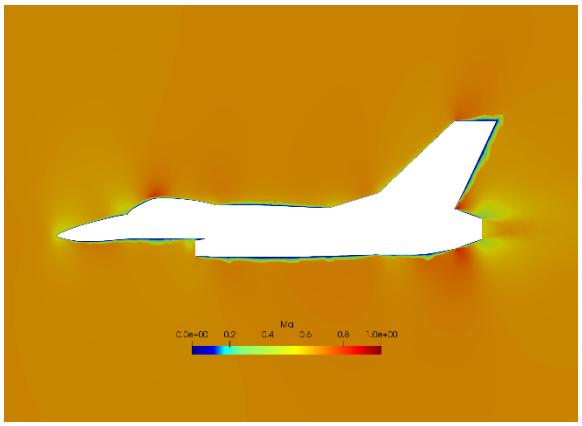

b

a: engine intake closed (no mass flow) *b*: engine intake open (with mass flow)

Figure 3. 26: Flow speed as Mach number over F16 side view at different engine intake conditions

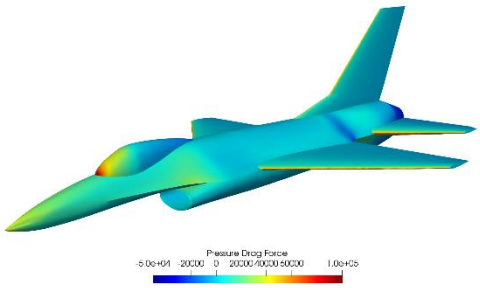

a

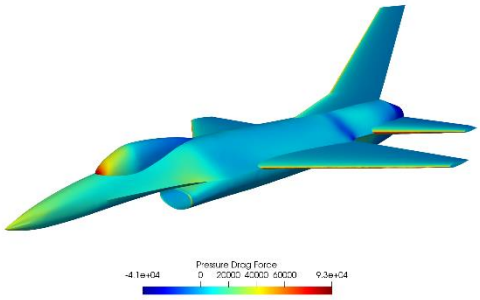

b

a : engine intake closed (no mass flow) *b*: engine intake open (with mass flow)

Figure 3. 27: Drag force distribution on the F16 at two different engine intake condition

4. FEASIBILITY AND COST ANALYSIS

In this study, mostly open-source software packages were used and not applicable to do cost analysis. Therefore, instead of cost analysis of the study, cost analysis of the flight of F16 and feasibility of F16 were made.

In the table 4.1, enhanced design was assumed a design that original design of the aircraft improved to create 5% less drag force and drag coefficient, C_d by optimizing the CFD results. This design may implement real life by applying surface improvement on the cockpit which has impact on drag force and coefficient or using diverterless engine intake design.

Table 4. 1: Analysis of the original and enhanced design

PR. / DESIGN	Drag Coefficient	Thrust Fuel Consumption ($g/N \cdot s$)	Fuel Consumption		Fuel Cost ($)	CO_2 Emission (kg/hr)
			$\left(\frac{kg}{hr}\right)$	$\left(\frac{lt}{hr}\right)$		
Normal	0.05891	59.2	328.7	410.8	535.19	1038.7
Enhanced	0.05596		312.2	390.3	428.2	986.8

As shown in the table 4.1, fuel consumption and fuel cost reduced. CO_2 emission is directly related with fuel consumption so with decreasing fuel consumption CO_2 emission decreased. At same time interval, enhanced design creates less emission and less fuel cost than original design.

On the other hand, F-16 which has enhanced design can fly 12 minutes more than original design of F-16. This is caused by less fuel consumption per hour which is directly related with drag force.

5. CONCLUSIONS AND FUTURE WORKS

5.1. Conclusion

In this presented study, F16 fighter aircraft's aerodynamics were analyzed with computational fluid dynamics to observe effects of altitude, Mach number, angle of attack and mass flow intake. Aerodynamics of the aircraft are affected by Mach number, angle of attack, temperature, and altitude. Simulations were run by using three different altitude, Mach number and angle of attack. Altitude change cannot directly take into account, but pressure is considered at relevant altitude. Pressure and temperature were changed at different altitudes and calculated by using NASA's atmosphere model. As temperature affects speed of sound Mach number changes if flow speed is not changed. To eliminate temperature effect, Mach number was kept constant at boundary conditions. Those factors could not be analyzed as a whole but analyzed separately. Only one factor was changed run-by-run. For example, to observe effects of altitude Mach number was hold constant and to observe effects of Mach number, altitude was hold constant.

SIMPLE algorithm was used as solution algorithm and density equation added to the algorithm for considering compressibility effects of air.

In the simulations in which speed is supersonic, shock waves were occurred and observed in the results. Shock waves affected the aerodynamics of the aircraft visibly in comparison with subsonic flow simulations. Altitude effect was also simulated at supersonic flight conditions. Moreover, simulations in which angle of attack were included were run at supersonic speed conditions. In the last section of the study mass flow inlet effect on aerodynamics of the aircraft was analyzed at subsonic speed flight. To conclude, altitude effects were analyzed at constant Mach number supersonic flight, Mach number effects were analyzed at constant altitude, angle of attack effects were analyzed at constant altitude and constant Mach number supersonic flight, and mass flow inlet were analyzed at constant altitude and constant Mach number subsonic flight. In real and experimental flight of the aircraft, those conditions can occur by cruise flight, accelerating flight, fast climb flight and wind tunnel test.

In this study, all cases were simulated using OpenFOAM open-source software. Mainly drag coefficient and pressure acting on the aircraft were investigated and flow fields around the aircraft are visualized. As a result, it was concluded that increasing altitude decreases C_d, increasing Mach number increases C_d, increasing angle of attack increases C_d and C_l with different behaviors and mass flow intake increases C_d.

5.2. Future Works

Aerodynamics of F16 will be analyzed using all effects together and more comprehensive results will be able to get obtained. Moreover, geometry of the aircraft will be created more real-like to obtain more precise results and more cells will be used to eliminate mesh related errors.

Optimization of the polar drag curve with fuel consumption, consumed fuel price and flight speed will be done. As a result of optimization, angle of attack will be found as optimum take off angle or climbing angle with minimum fuel consumption and flight cost.

REFERENCE

[1] Akgün, O., Golcuk, A. İ., Kurtuluş, D. F., & Kaynak, Ü. (2016 0). *Drag Analysis of a Supersonic Fighter Aircraft*. Ninth International Conference on Computational Fluid Dynamics (ICCFD9), Istanbul, TURKEY. https://hdl.handle.net/11511/79292

[2] Babitha Kodavanla Et Al., B. K. E. A. (2018). CFD Analysis of F-16 Falcon. *International Journal of Mechanical and Production Engineering Research and Development*, *8*(2), 1293–1302. https://doi.org/10.24247/ijmperdapr2018149

[3] *Aerodynamic Characteristics of Forebody and Nose Strakes Based on F-16 Wind Tunnel Test Experience*. (1979). NASA. https://ntrs.nasa.gov/api/citations/19790019972/downloads/19790019972.pdf

[4] *Supersonic Aerodynamic Characteristics of an Advanced F-16 Derivative Aircraft Configuration*. (1993). NASA. https://ntrs.nasa.gov/api/citations/19930022544/downloads/19930022544.pdf

[5] Boelens, O. J., & Luckring, J. M. (2014). Flow Analysis of the F-16XL Aircraft (CAWAPI-2) At Transonic Flow Conditions. *52nd Aerospace Sciences Meeting*. https://doi.org/10.2514/6.2014-0757

[6] Sharma, M., & Reddy, T.R. (2013). Flow Analysis over an F-16 Aircraft Using Computational Fluid Dynamics.

[7] A., A., & A. (2012, January 10). *OpenVSP*. OpenVSP Website. Retrieved June 12, 2022, from http://openvsp.org/

[8] Greenshields, C. (2021, July 13). *OpenFOAM v8 User Guide*. OpenFOAM. Retrieved June 12, 2022, from https://cfd.direct/openfoam/user-guide-v8/

[9] *Gmsh 4.10.3*. (2022, March 26). Gmsh Documentation. Retrieved June 12, 2022, from https://gmsh.info/doc/texinfo/gmsh.html

[10] *Earth Atmosphere Model - Metric Units*. (2022b). NASA. Retrieved June 12, 2022, from https://www.grc.nasa.gov/www/k-12/airplane/atmosmet.html

[11] Rao, S. S. (2009). *Engineering Optimization: Theory and Practice* (4th ed.). Wiley.

[12] *ParaView User's Guide — ParaView Documentation 5.10.0 documentation*. (2020). ParaView. Retrieved June 12, 2022, from https://docs.paraview.org/en/latest/UsersGuide/index.html

APPENDICES

Appendix 2-2

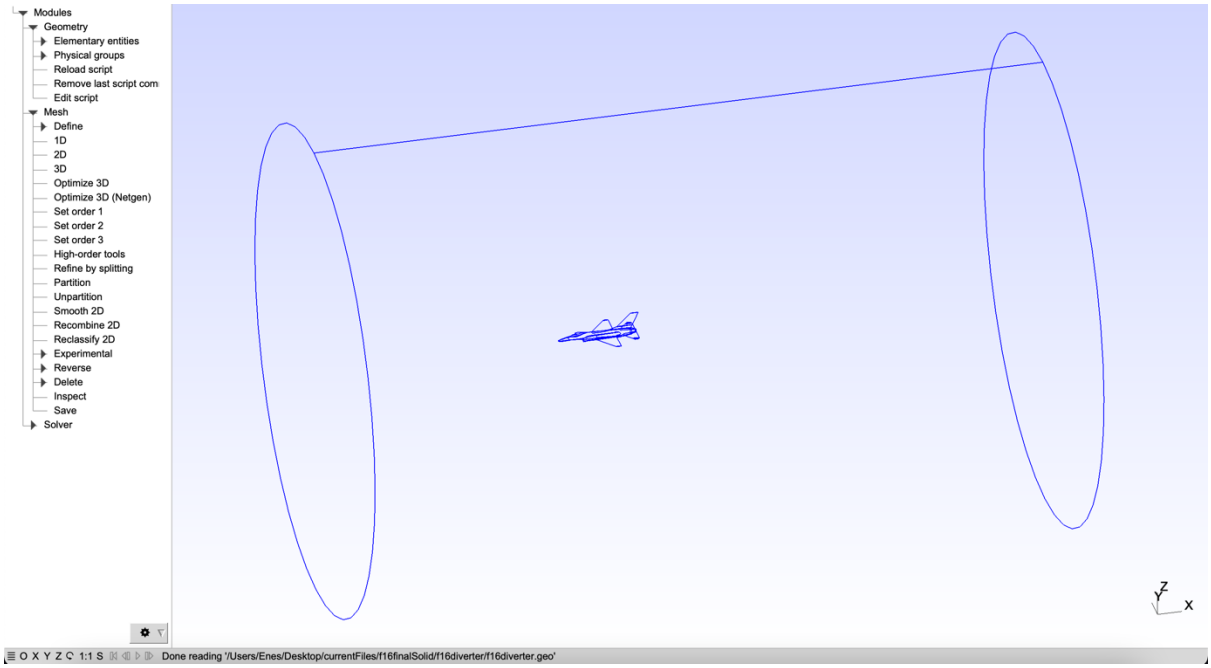

Figure A. 1: GMSH .geo file ouput

Table A. 1: OpenFOAM dimensions table

No.	Property	SI unit	USCS unit
1	Mass	kilogram (kg)	pound-mass (lbm)
2	Length	metre (m)	foot (ft)
3	Time	second (s)	second (s)
4	Temperature	Kelvin (K)	degree Rankine (°R)
5	Quantity	mole (mol)	mole (mol)
6	Current	ampere (A)	ampere (A)
7	Luminous intensity	candela (cd)	candela (cd)

Appendix 2-3

```
//MATLAB Code using NASA equations for earth atmosphere model
Altitude(1) = 0;
for i = 1:16
   Altitude(i+1) = Altitude(i) + 1000;
   if Altitude(i) <= 11000; %troposphere
      Temperature(i) = 15.04 - 0.00649*Altitude(i);
      Pressure(i) = 101.29*(((Temperature(i)+273.1)/288.08)^5.256);
   else %stratosphere
      Temperature(i) = -56.46;
      Pressure(i) = 22.65*exp(1.73-0.000157*Temperature(i));
   end
   Rho(i) = Pressure(i)/(0.2869*(Temperature(i)+273.1));
   i = i + 1;
end
```

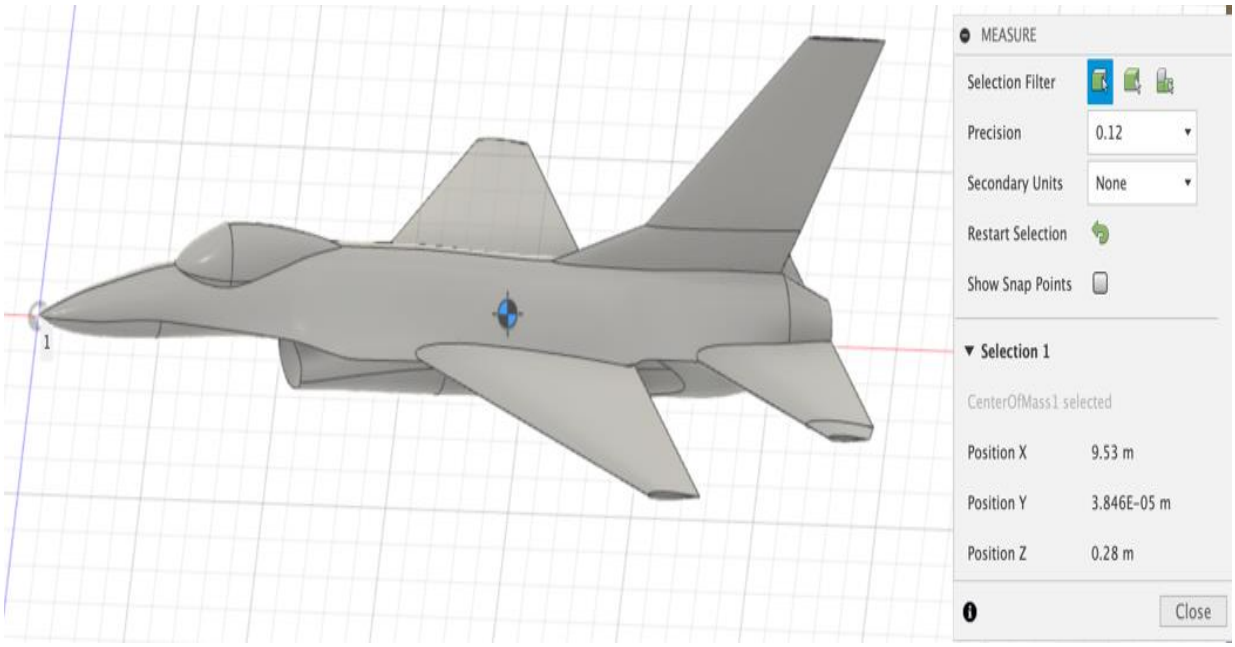

Figure A. 2: Center of gravity position of F16 model

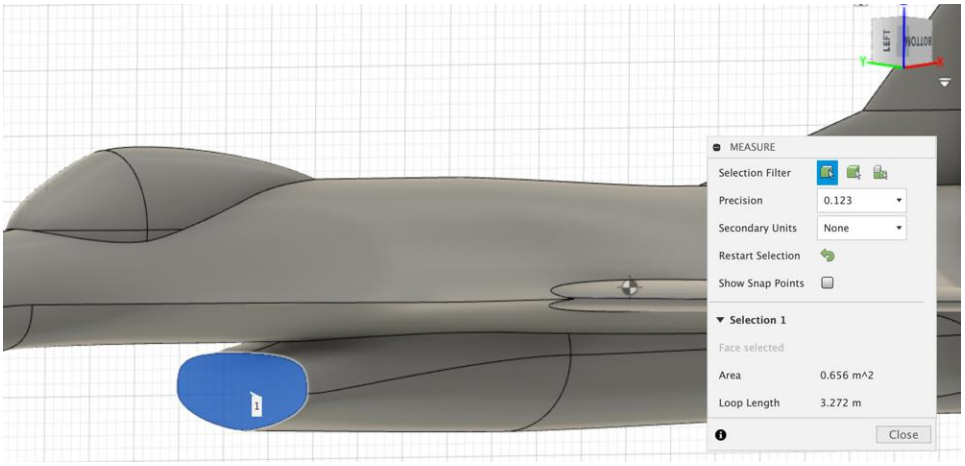

Figure A. 3: Engine intake area of F16 model

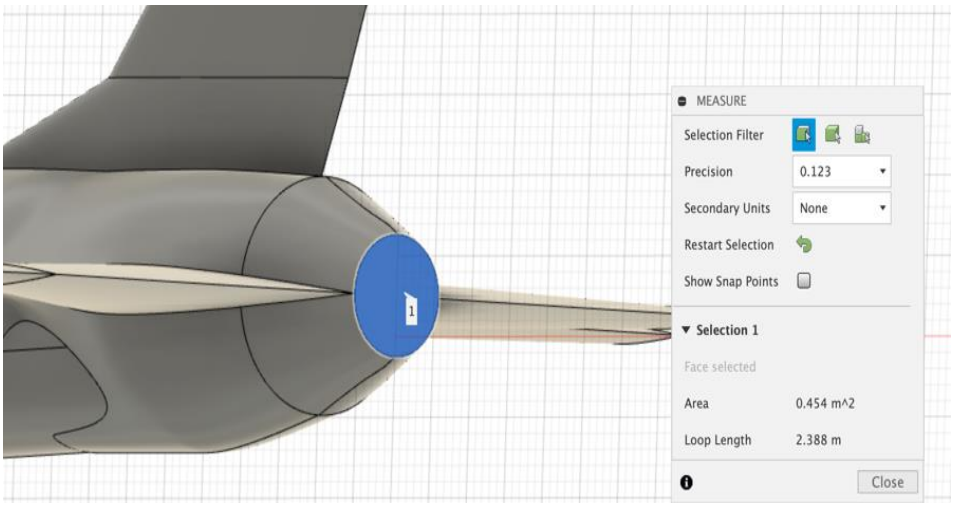

Figure A. 4: Engine outlet area of F16 model

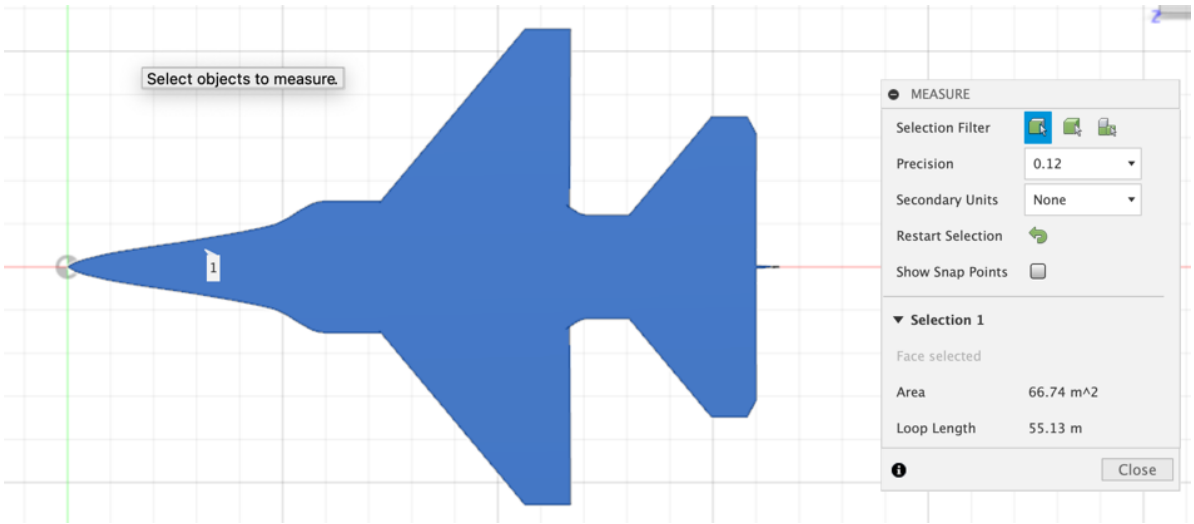

Figure A. 5: Planform area of F16 model